Data-Driven Techniques for Monthly Pan Evaporation Modeling in Iraq

Jazuli Abdullahi[1] & Ala Tahsin[2]

[1]Department of Civil Engineering, Faculty of Civil and Environmental Engineering, Near East University, Nicosia, Cyprus
[2] Department of Civil Engineering, Faculty of Engineering, Tishk International University, Iraq
Correspondence: Jazuli Abdullahi, Near East University, Nicosia, Cyprus.
Email: jazulibinabdallah@gmail.com

Doi: 10.23918/eajse.v6i1p104

Abstract: Evaporation plays significant roles in agricultural production, climate change and water resources management. Hence, its accurate prediction is of paramount importance. This study aimed at investigating the potentials of artificial neural network (ANN), support vector regression (SVR) and classical multiple linear regression (MLR) models for monthly pan evaporation modeling in Erbil and Salahaddin stations of Iraq. Data including maximum, minimum, and mean temperatures, wind speed, relative humidity, and vapor pressure were used as inputs for 5 different input combinations to achieve the study objective. For performance evaluation of the applied models, root mean square error (RMSE) and determination coefficient (DC) were employed. In addition, Taylor diagrams were plotted to compare the performance of the models. The results showed that models with 6 inputs provided the best performance for Salahaddin station, but 5 inputs model led to better accuracy for MLR model in Erbil station. ANN provided superior performance with DC = 0.9527 and RMSE = 0.0660 for Erbil station while for Salahaddin station, SVR performed better with DC and RMSE of 0.8487 and 0.0753 in the validation phase. The general study results demonstrated that all the 3 applied models could be employed for successful pan evaporation modeling in the study stations, but for better accuracy, ANN is preferable.

Keywords: Artificial Neural Network, Support Vector Regression, Erbil, Data, Salahaddin

1. Introduction

Pan evaporation (Ep) is extensively used in irrigation as well as regional water resources systems design being a significant factor for atmospheric evaporative demand (Azorin-Molina et al., 2015). It plays an important role in the global climate change context with respect to energy cycles and water balance (Yang & Yang, 2012; Wang et al., 2017). Analyses on the causes and trends of Ep have been carried out in different regions of the world by many studies including Zhang et al. (2015), yet, it is generally recognized that in some areas (more especially arid and semiarid regions which have scarce water resources), evaporation is among the hydrologic water cycle components with less understanding pattern (Valipour & Eslamian, 2014; Goyal et al., 2014). For agricultural production, irrigation control and water resources management, accurate estimation of Ep is of great priority (Shiri et al., 2014).

Direct and indirect approaches are generally the two methods used for calculating or predicting evaporation. The direct method employed the use of instruments for measuring the evaporation (such as Ep); however, practical issues such as maintenance and measurement errors as well as instrumental limits may deter the efficiency of the evaporation measurements (Wang et al., 2017). Hence, for the evaporation prediction, several methods using observed meteorological parameters have been proposed by modeling the relationship linearly between Ep and meteorological data (including solar radiation, sunshine hours, air pressure, relative humidity, air temperature, etc.) (Wang et al., 2017). The empirical methods when applied to other sites however need to be recalibrated. The evaporation

process is however nonlinear, unsteady, incidental and complex (Kisi, 2015). Therefore, driven accurate relationship that will represent the physical processes involved between climatic parameters and Ep is difficult to be achieved (kim et al., 2015). Consequently, the use of nonlinear data driven methods for hydrological modeling studies on Ep have been emphasized by many researchers (Wang et al., 2017).

Recently, application of artificial intelligence (AI) methods such as artificial neural network (ANN) and support vector regression (SVR) have been widely recognized for ecohydrological process modeling across the globe (Bewoor et al., 2016). For instance, Rahimikhoob (2009) estimated Ep in daily basis in a semiarid environment using ANN as a function of air temperature in the southwest of Iran. Shirsath and Singh (2010) applied ANN, MLR and climate-based models for daily pan evaporation estimation. Wang et al. (2017) used four heuristic approaches including least square-SVR and MLR for daily pan evaporation estimation in Dongting Lake Basin, China. Qasem et al. (2019) modeled monthly pan evaporation using ANN, SVR and their hybrid forms.

Despite the significance of using AI techniques in modeling evaporation process which is an important parameter in irrigation system, water resources management and hydrologic water cycle, based on the overall assessment of the authors, there is no study in the present literature that used ANN, SVR and MLR models for monthly pan evaporation modeling in Erbil and Salahaddin stations in particular and Iraq in general. Therefore the main aim of this study was to evaluate the performance of ANN, SVR and MLR models using different input combinations of meteorological parameters (including maximum temperature, minimum temperature, mean temperature, relative humidity, vapor pressure and wind speed) for monthly Ep modeling.

2. Materials and Method

2.1 Study Locations and Data

Erbil is the largest and the capital city of Kurdistan region in northern Iraq. Its location is within a continental semiarid climate. Erbil experiences cool and rainy winters with warm and dry summers (Nourani et al., 2019a). Erbil governorate estimated population in 2010 was 1,820,000 whereas the city population was 852,000. The Erbil district population density in terms of persons/km^2 was 472.9 (Rasul et al., 2015). Salahaddin city is also located in Kurdistan region in further north of Iraq. The climate of Salahaddin is considered semiarid according to Sarlak and Agha (2018) study. Figure 1 shows map of Iraq and respective study locations.

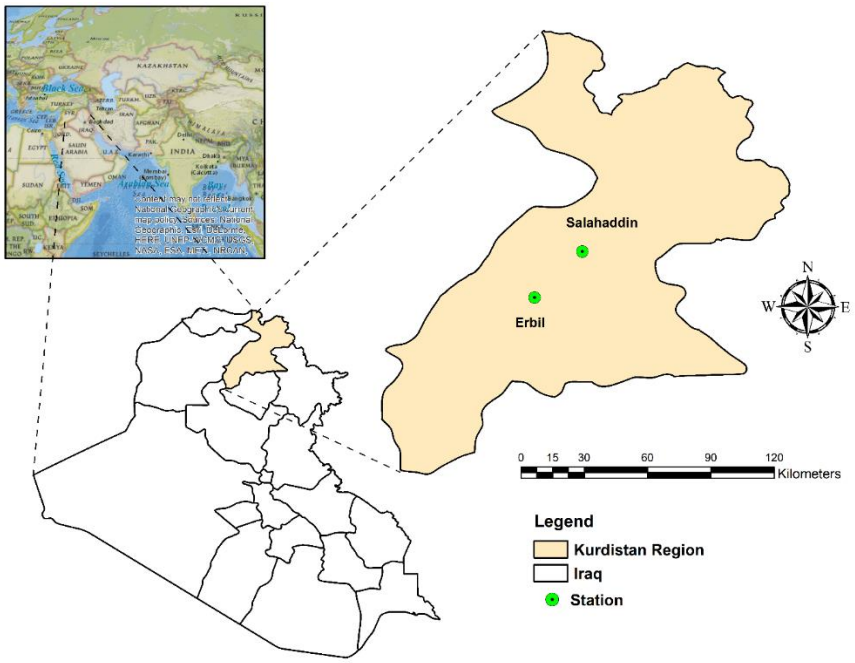

Figure 1: Study country and location of the study stations

The data used in this study are of 20 years duration (1992-2011) of monthly measurement including maximum temperature (T_{max}), minimum temperature (T_{min}), mean temperature (T_{mean}), relative humidity (R_H), vapor pressure (V_P), Ep and wind speed (U_2) obtained for each study station from general directorate of dams and reservoirs, Kurdistan. Table 1 gives statistical description of the used data.

Table 1: Data descriptive statistics

Station	Variable	unit	Minimum	Maximum	Mean	St.deviation
Erbil	T_{mean}	^0C	6	37.3	21.28	9.37
	T_{max}	^0C	9.5	45	27.5	10.63
	T_{min}	^0C	0.6	30	15.07	8.26
	R_H	%	5	88	46.73	18.78
	V_P	mbar	3.5	18.3	11.12	2.57
	U_2	m/s	1	7	2.5	0.8
	Ep	mm/day	1	16	6.84	4.39
Salahaddin	T_{mean}	^0C	0	34.6	18.02	9.27
	T_{max}	^0C	0	39.9	22.26	10.29
	T_{min}	^0C	-1.6	29.2	13.35	8.57
	R_H	%	24	92	52.27	16
	V_P	mbar	4.7	20.1	10.46	3.58
	U_2	m/s	1	4	2.36	0.64
	Ep	mm/day	0.1	15.5	4.99	3.48

As seen in Table 1, Erbil station is more semiarid which has T_{max} as high as 45 ^{0}C and R_H as low as 5% whereas Salahaddin is more humid with T_{max} as 39.9 ^{0}C and maximum R_H of 92%. Evaporation is less in Salahaddin station as minimum Ep value of 0.1 mm/day could be seen. This is because of the dryness of the Erbil land coupled with high temperature which increase the rate of Ep for Erbil station. To determine the effect and correlation of each variable on the target, Pearson correlation matrix was developed. Table 2 provides the results of the used correlation matrix.

Table 2: Results of the applied correlation matrix

Station	Variable	Ep (mm/day)	T_{mean} ^{0}C	T_{max} ^{0}C	T_{min} ^{0}C	R_H (%)	V_P (mbar)	U_2 (m/s)
Erbil	Ep (mm/day)	1						
	T_{mean} ^{0}C	0.95187	1					
	T_{max} ^{0}C	0.947304	0.99118	1				
	T_{min} ^{0}C	0.948491	0.989551	0.971483	1			
	R_H (%)	-0.86684	-0.88408	-0.89572	-0.86305	1		
	V_P (mbar)	0.725395	0.778229	0.762167	0.792531	-0.54576	1	
	U_2 (m/s)	0.000203	-0.03324	-0.02856	-0.04811	0.027797	0.001558	1
Salahaddin	Ep (mm/day)	1						
	T_{mean} ^{0}C	0.886293	1					
	T_{max} ^{0}C	0.887104	0.981548	1				
	T_{min} ^{0}C	0.903824	0.982538	0.990335	1			
	R_H (%)	-0.88738	-0.87041	-0.88985	-0.88183	1		
	V_P (mbar)	0.786193	0.871481	0.873193	0.889176	-0.69521	1	
	U_2 (m/s)	0.240498	0.098463	0.074705	0.106517	-0.16363	0.042088	1

The results shown in Table 2 demonstrated that the correlation between Ep and temperature is directly proportional, implying that as the temperature increases the rate of Ep increases and vice versa. This is why the temperatures (T_{mean}, T_{max}, and Tmin) in Erbil station have higher correlation than in Salahaddin station. Among all the variables, R_H was found to be less correlated with Ep compared to the rest.

2.2 Data Normalization and Performance Criteria

At initial stage, the data were normalized to eliminate the dimension of inputs and output and to ensure equal attention is given to all variables. The data were normalized between 0 and 1 according to Elkiran et al. (2018) as.

$$Ep_{norm} = \frac{Ep_i - Ep_{min}}{Ep_{max} - Ep_{min}} \quad [1]$$

Where Ep_{norm}, Ep_i, Ep_{max} and Ep_{min} are respectively the normalized, observed, maximum and minimum values of Ep.

To determine the accuracy of the applied models, this study endorsed Legates and McCabe (1999) study which suggested that for any hydroclimatic model, Determination Coefficient (DC) and Root Measn Square Error can be sufficient for performance evaluation (Nourani et al., 2019a), given by;

$$DC = 1 - \frac{\sum_{i=1}^{N}(Ep_i - \widehat{Ep}_i)^2}{\sum_{i=1}^{N}(Ep_i - \overline{Ep}_i)^2} \quad [2]$$

$$RMSE = \frac{\sum_{i=1}^{N}(Ep_i - \widehat{Ep}_i)^2}{N} \quad [3]$$

Where Ep_i has been defined, N, $\widehat{Ep}_i$, and $\overline{Ep}_i$ are the number of observations, predicted values and mean of the observed values, respectively. The DC ranges between - ∞ to 1 and RMSE between 0 to ∞ with DC towards 1 and RMSE close to 0 imply high efficiency (Nourani et al., 2019b).

2.3 Proposed Methodology

In this study, AI based and MLR models were applied for modeling Ep in two meteorological stations in Iraq. At initial stage, correlation matrix was applied to determine the effectiveness of the variables on Ep. Based on the obtained results, five different input combinations were formed given as.

$$Ep^s = f(T^s_{min}, T^s_{mean}) \quad [4]$$

$$Ep^s = f(T^s_{min}, T^s_{mean}, T^s_{max}) \quad [5]$$

$$Ep^s = f(T^s_{min}, T^s_{mean}, T^s_{max}, V^s_p) \quad [6]$$

$$Ep^s = f(T^s_{min}, T^s_{mean}, T^s_{max}, V^s_p, U^s_2) \quad [7]$$

$$Ep^s = f(T^s_{min}, T^s_{mean}, T^s_{max}, V^s_p, U^s_2, R^s_H) \quad [8]$$

Where the superscript s (such as in Ep^s) represents the station (e.g. Erbil or Salahaddin), $T_{min}, T_{mean}, T_{max}, V_p, U_2$ and R_H were previously defined. The general methodology employed in this study is given in Fig 2.

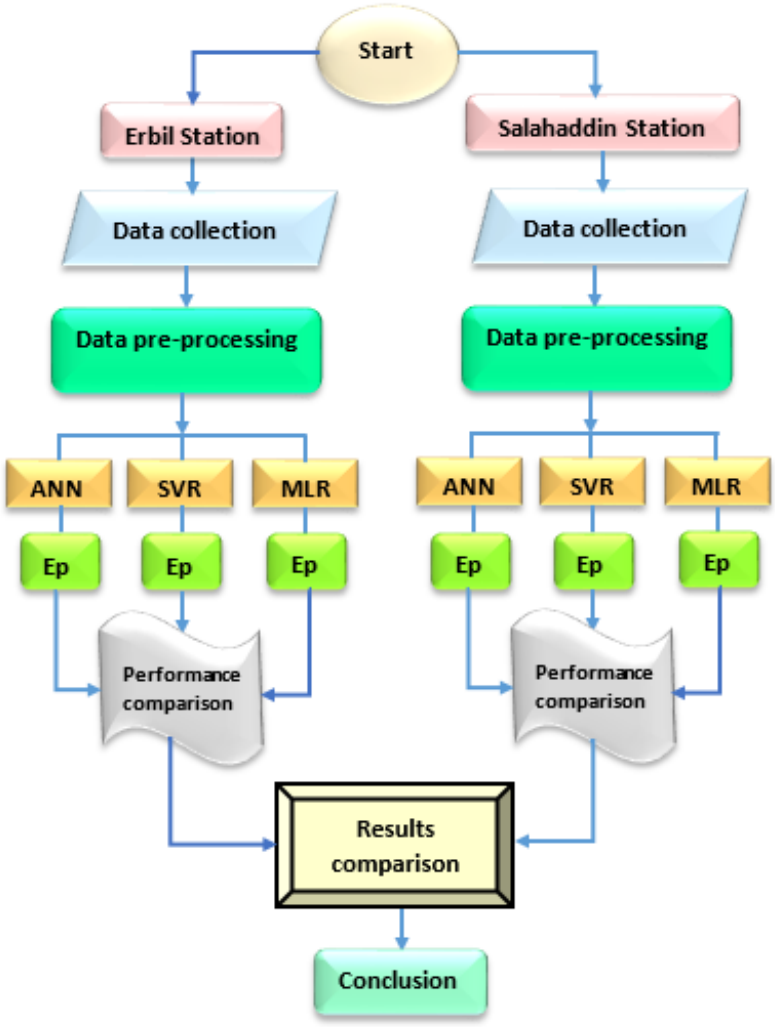

Figure 2: The overall methodology of the study

2.4 Model Validation

A stratified *k*-fold cross validation was applied in this study. The main advantages of using this validation approach over hold-out validation approach (which uses single test set per station) are that both training and validation are done by all observations and each observation is used exactly once for the model validation (Nourani et al., 2019a). The data were randomly divided into *4*-folds of equal subsamples as shown in Fig.4. The model was trained using ¾ of the subsamples while the remaining ¼ was used for testing the model. The procedure was repeated 4 times (the number of subsamples), in each case, different *k*-1 (*4*-1) subsamples were used for training and the remaining subsample for testing the model. Figure 3 shows the data splitting procedure for training and validation of the models.

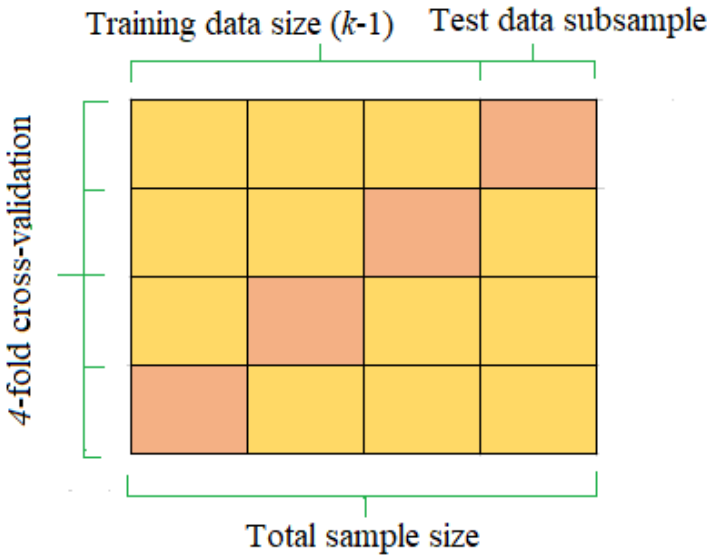

Figure 3: Data division for the applied *k*-fold cross validation

2.5 Artificial Neural Network (ANN)

ANN provides a determined approach in dealing with non-linear, noisy, and dynamic data, more specifically when the physical fundamental relationship are not completely known (Nourani et al., 2012).

ANN constitutes a number of simple processing elements that are interconnected by nodes or neurons with fascinating characteristics of information processing including parallelism, nonlinearity, generalization capability, learning and noise tolerance. For solving many engineering problems, a feed forward neural network trained with back propagation (FFBP) algorithm is the most applied ANN method (Nourani et al., 2009; Abdullahi et al., 2017). The FFBP method is comprised of layers of parallel processing elements known as neurons, with every successive layer neuron completely connected to its predecessor layer by weight (Abdullahi & Elkiran, 2017). BP algorithm generally accomplished this ANN learning (Hornik et al., 1989). Figure 4 shows the ANN structure with 4 inputs, 5 hidden layer neurons and an output (Ep).

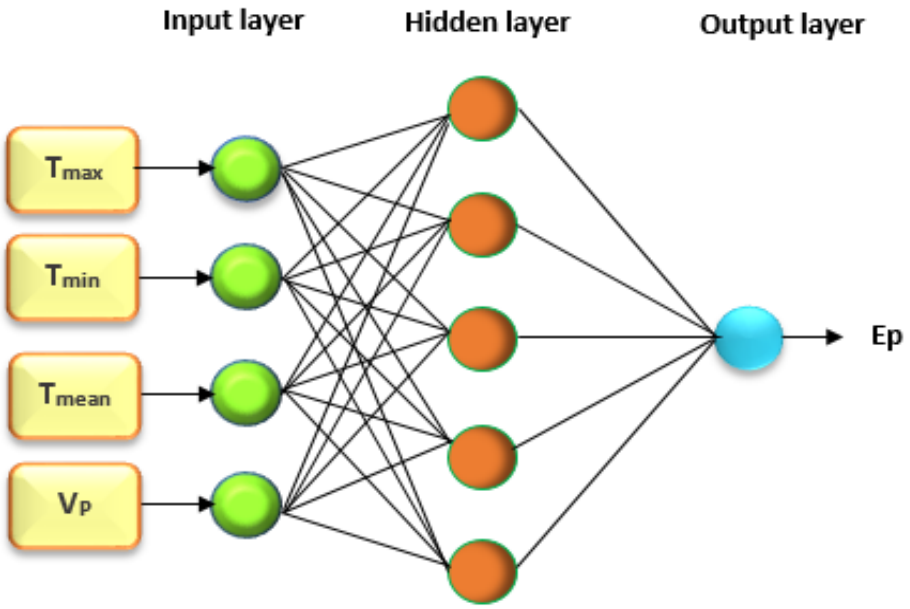

Figure 4: A three layered FFNN structure

2.6 Support Vector Regression (SVR)

The concept of SVM learning was introduced by Cortes and Vapnik (1995). It presents a satisfactory approach to the problems of classification, pattern recognition, regression and prediction. SVM based methods such as SVR is different from many other black box methods, in such a way that instead of minimizing the error between predicted and observed values, the operational risk is considered as the objective function to be minimized. A linear regression is fitted first on the data in SVR, and then to catch the nonlinear data pattern, the output go through a nonlinear kernel.

Given a set of training data $\{(x_i, d_i)\}$ d_i is the actual value, x_i is the input vector and N is the data patterns total number), the general SVR function is (Wang et al., 2013):

$$y = f(x) = w\varphi(x_i) + b \qquad [4]$$

where $\varphi(x_i)$ non-linearly mapped from input vector *x* which implies feature spaces (Vapnik 1998). minimization of the objective function and assigning positive values for the slack parameters of ξ and ξ* may determine regression parameters of *b* and *w* (Wang et al., 2013).

Minimize: $\frac{1}{2} \| w \|^2 + C[\sum_i^N (\xi_i + \xi_i^*)]$

Subject to: $\begin{cases} w_i\varphi(x_i) + b_i - d_i \le \varepsilon + \xi_i^* \\ d_i - w_i\varphi(x_i) + b_i \le \varepsilon + \xi_i^* \\ \xi_i, \xi_i^* \end{cases}$ i=1,2,…,N

where $\frac{1}{2} \| w \|^2$ is the weights vector norm and the trade-off between the regularized term and the empirical error is determined by C referred to as the regularized constant? ε is equivalent to the approximation accuracy placed within the training data points and is called the tube size. By defining Lagrange multipliers αi and αi*, optimization problem mentioned can be changed to the dual quadratic

optimization problem. After solving the quadratic optimization problem, vector w in Eq. (9) can be computed as (Wang et al., 2013):

$$w^* = \sum_{i=1}^{N}(\alpha_i - \alpha_i^*)\varphi(x_i) \quad [9]$$

So, SVR can be expressed in the final form of as (Wang et al., 2013):

$$f(x, \alpha_i, \alpha_i^*) = \sum_{i=1}^{N}(\alpha_i - \alpha_i^*)K(x, x_i) + b \quad [10]$$

b is bias term and non-linear mapping into feature space is performed by k (xi, xj) which is the kernel function. Gaussian Radial Basis Function (RBF) kernel is one of the commonly used kernel functions as (Haghiabi et al. 2017):

$$k(x_1, x_2) = \exp(-\gamma||x_1 - x_2||^2) \quad [11]$$

where, γ is the kernel parameter. Figure 5 show the SVR structure.

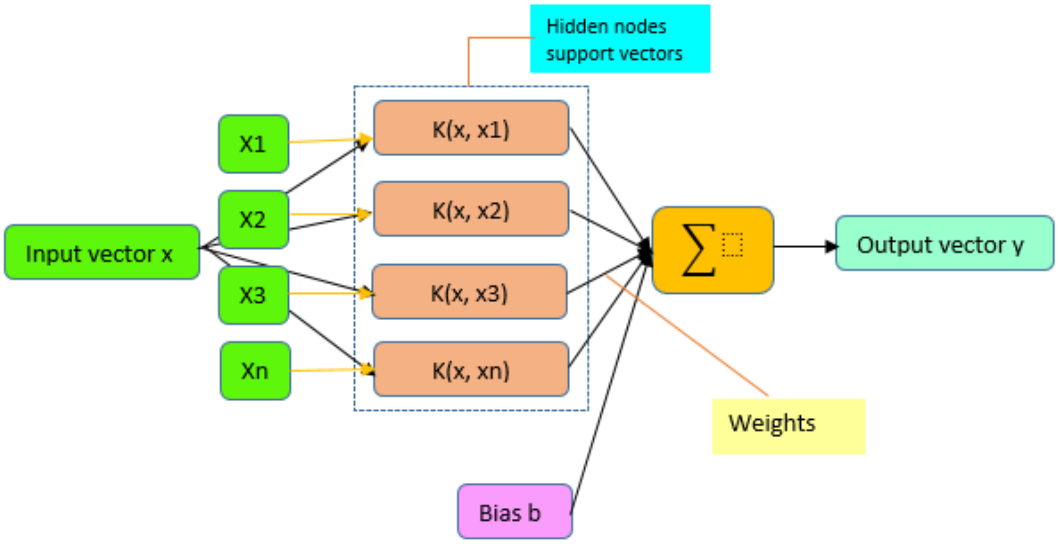

Figure 5: The structure of SVM model (Ghorbani et al., 2018)

2.7 Multiple Linear Regression

Multiple linear regression (MLR) is a famous method of modeling mathematically, the linear relationship between one or more independent variables and dependent variable. In general, the dependent variable y, and n regressor variables may be related by (Elkiran et al., 2018):

$$y = b_0 + b_1x_1 + b_2x_2 + b_3x_3 + \cdots + b_ix_i + \xi \quad [12]$$

Where x_i is the value of the i^{th} predictor, b_0 is the regression constant, and b_i is the coefficient of the i^{th} predictor and ξ is the error term.

3. Results and Discussion

This study was performed to model Ep for Erbil and Salahaddin stations in the Kurdistan region of Iraq, hence the results and discussion section is provided accordingly. For the ANN model in both stations, FFNN was used for the model training using Levenberg Marquardt (LM) algorithm. Single hidden layer was used and via trial and error, the best number of hidden layer neurons was selected. For SVR modeling, RBF kernel shows better accuracy and hence used in this study (Sharghi et al., 2018). Lastly, based on input-output linear relationship, MLR modeling of Ep was performed. Table 3 shows the results of applied models for Erbil station.

Table 3: Results of Ep modeling for Erbil station

				Training		Validation	
Model	Model No.	Input	Structure	DC	RMSE	DC	RMSE
ANN	M1	T_{min}, T_{mean}	2-7-1	0.9215	0.0803	0.9042	0.0938
	M2	T_{max}, T_{min}, T_{mean}	3-6-1	0.9444	0.0675	0.8906	0.1003
	M3	T_{max}, T_{min}, T_{mean}, V_P	4-12-1	0.9385	0.0711	0.9268	0.0820
	M4	T_{max}, T_{min}, T_{mean}, V_P, U_2	5-15-1	0.9417	0.0692	0.9376	0.0757
	M5	T_{max}, T_{min}, T_{mean}, V_P, U_2, R_H	6-14-1	0.9506	0.0637	0.9527	0.0660
SVR	M1	T_{min}, T_{mean}	RBF	0.9236	0.0792	0.8988	0.0964
	M2	T_{max}, T_{min}, T_{mean}	RBF	0.9282	0.0768	0.9098	0.0910
	M3	T_{max}, T_{min}, T_{mean}, V_P	RBF	0.9290	0.0763	0.9120	0.0899
	M4	T_{max}, T_{min}, T_{mean}, V_P, U_2	RBF	0.9301	0.0758	0.9154	0.0882
	M5	T_{max}, T_{min}, T_{mean}, V_P, U_2, R_H	RBF	0.9360	0.0725	0.9155	0.0881
MLR	M1	T_{min}, T_{mean}	2-1	0.9104	0.0858	0.8915	0.0998
	M2	T_{max}, T_{min}, T_{mean}	3-1	0.9110	0.0855	0.8979	0.0969
	M3	T_{max}, T_{min}, T_{mean}, V_P	4-1	0.9122	0.0849	0.9036	0.0941
	M4	T_{max}, T_{min}, T_{mean}, V_P, U_2	5-1	0.9132	0.0844	0.9054	0.0932
	M5	T_{max}, T_{min}, T_{mean}, V_P, U_2, R_H	6-1	0.9148	0.0836	0.9030	0.0944

The data have been normalized, so RMSE has no unit

For the structure of ANN model in Table 3, a-b-c represent the number of inputs, number of hidden layer nodes and number of outputs. For SVR, RBF stands for tuned kernel's parameters used in SVR construction and x-y for MLR model signifies inputs and output number, respectively.

In view of the obtained results in Table 3, it is apparent that all the applied models are sufficient for Ep modeling in Erbil station with DC and RMSE up to 0.9527 and 0.0660 for ANN model, 0.9155 and 0.0881 for SVR model and 0.9054 and 0.0932 for MLR model in the validation phase for the best performance models. Also, from Table 3, it can be seen that the AI models have superior performance over MLR model both in training and validation phases. This could be attributed to the ability of AI techniques to deal with complex and nonlinear Ep process. Among the AI models, ANN is found to have better prediction accuracy, though fluctuations could be observed such as in M2 where better performance is achieved by SVR model using both DC and RMSE performance indicators in the validation phase. Many reasons could be associated to this development some of which include.

1. Time series prediction involved complex and uncertain behavior of a system due to the huge amount of data used for a long period of time, which could be affected by seasonality, non-stationarity and missing values. This could result in increase and decrease (or rise and fall) of the observations, which in turn might lead to failure of a particular model to capture all the aspects of the data efficiently. As such, one model may perform better at certain stage and inferior at another stage of the modeling.
2. Though the applied models are both nonlinear in nature, but their methodologies of application as well as the training parameters are quite different, thus an adjustment of a particular parameter may increase accuracy of one model and could be deterrent to another.

Figure 6 shows the time series and scatter plots for the best performance models in the validation phase of Erbil station.

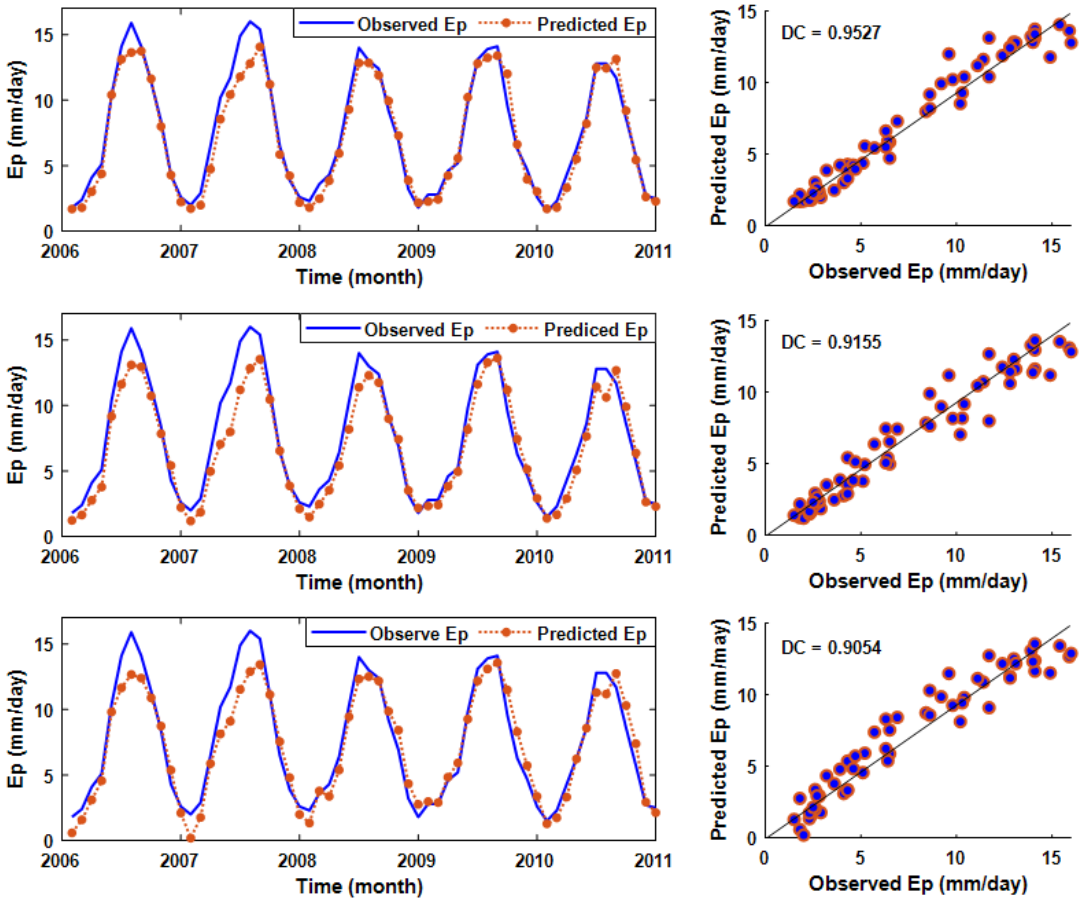

Figure 6: Time series and scatter plots for the best performance models in Erbil station for (a) ANN model (b) SVR model (c) MLR model

Table 4 shows the results of applied models for Salahaddin station. Both the models applied and structure are same as in the case of Erbil station.

Table 4: Results of Ep modeling for Salahaddin station

				Training		Validation	
Model	Model No.	Input	Structure	DC	RMSE	DC	RMSE
ANN	M1	T_{max}, T_{mean}	2-4-1	0.8519	0.0648	0.7356	0.1236
	M2	T_{max}, T_{min}, T_{mean}	3-5-1	0.8612	0.0627	0.8004	0.1074
	M3	T_{max}, T_{min}, T_{mean}, V_P	4-11-1	0.8192	0.1022	0.7699	0.0808
	M4	T_{max}, T_{min}, T_{mean}, V_P, U_2	5-10-1	0.9053	0.0518	0.7944	0.1090
	M5	T_{max}, T_{min}, T_{mean}, V_P, U_2, R_H	6-16-1	0.8776	0.0589	0.8473	0.0753
SVR	M1	T_{min}, T_{mean}	RBF	0.8111	0.0732	0.7775	0.1134
	M2	T_{max}, T_{min}, T_{mean}	RBF	0.8210	0.0713	0.7788	0.1130
	M3	T_{max}, T_{min}, T_{mean}, V_P	RBF	0.8356	0.0683	0.7776	0.1134
	M4	T_{max}, T_{min}, T_{mean}, V_P, U_2	RBF	0.8846	0.0572	0.7889	0.1104
	M5	T_{max}, T_{min}, T_{mean}, V_P, U_2, R_H	RBF	0.9041	0.0522	0.8487	0.0935
MLR	M1	T_{min}, T_{mean}	2-1	0.7880	0.1107	0.7235	0.0886
	M2	T_{max}, T_{min}, T_{mean}	3-1	0.7888	0.1104	0.7249	0.0883
	M3	T_{max}, T_{min}, T_{mean}, V_P	4-1	0.7894	0.1103	0.6943	0.0931
	M4	T_{max}, T_{min}, T_{mean}, V_P, U_2	5-1	0.8003	0.1074	0.8003	0.0851
	M5	T_{max}, T_{min}, T_{mean}, V_P, U_2, R_H	6-1	0.8618	0.0626	0.8301	0.0825

The data have been normalized, so RMSE has no unit

Being semiarid climate stations, the results in Table 4 show similar characteristics to the results obtained for Erbil station. It can be seen that for all the applied models, the performance of the models increases as the number of inputs increases. This shows that evaporation process has a complex stochastic nature which its accurate prediction requires several climatological parameters and depends on many factors. Despite the existence of strong correlation between Ep and temperatures, more variables are needed for efficient Ep modeling. For example, comparing M1 (which has only T_{min}, and T_{mean}) with M5 (which has T_{max}, T_{min}, T_{mean}, V_P, U_2, and R_H) a difference in performance in terms of DC up to 11% could be achieved for ANN models in the validation phase.

Comparing Tables 3 and 4 results for Erbil and Salahaddin stations it can be deduced that, the applied models provided better performances in Erbil station than in Salahaddin station despite having same semiarid climate. This is because evaporation has a direct relationship with temperature. As shown in Table 1, the T_{max}, T_{min}, and T_{mean} are all higher in Erbil station than in Salahaddin station, hence as the temperature increases the rate of evaporation increases, hence higher Ep prediction by the models. However, behavior of the climate between the stations may lead to higher results in Erbil than Salahaddin. For instance, Sarlak and Agha (2018) study shows that different aridity index and period of investigation give varied climate for Salahaddin station. Using UNEP (1992) aridity index, Salahaddin station was found to be semiarid between 1998 – 2011, subhumid between 1980 – 1997 and subhumid between 1980 – 2011. The unrealistic nature of the climate in the station leads to inefficiency of models to give comparable performance with the results of Erbil station. Figure 7 shows the time series and scatter plots for the best performance models in the validation phase of Salahaddin station.

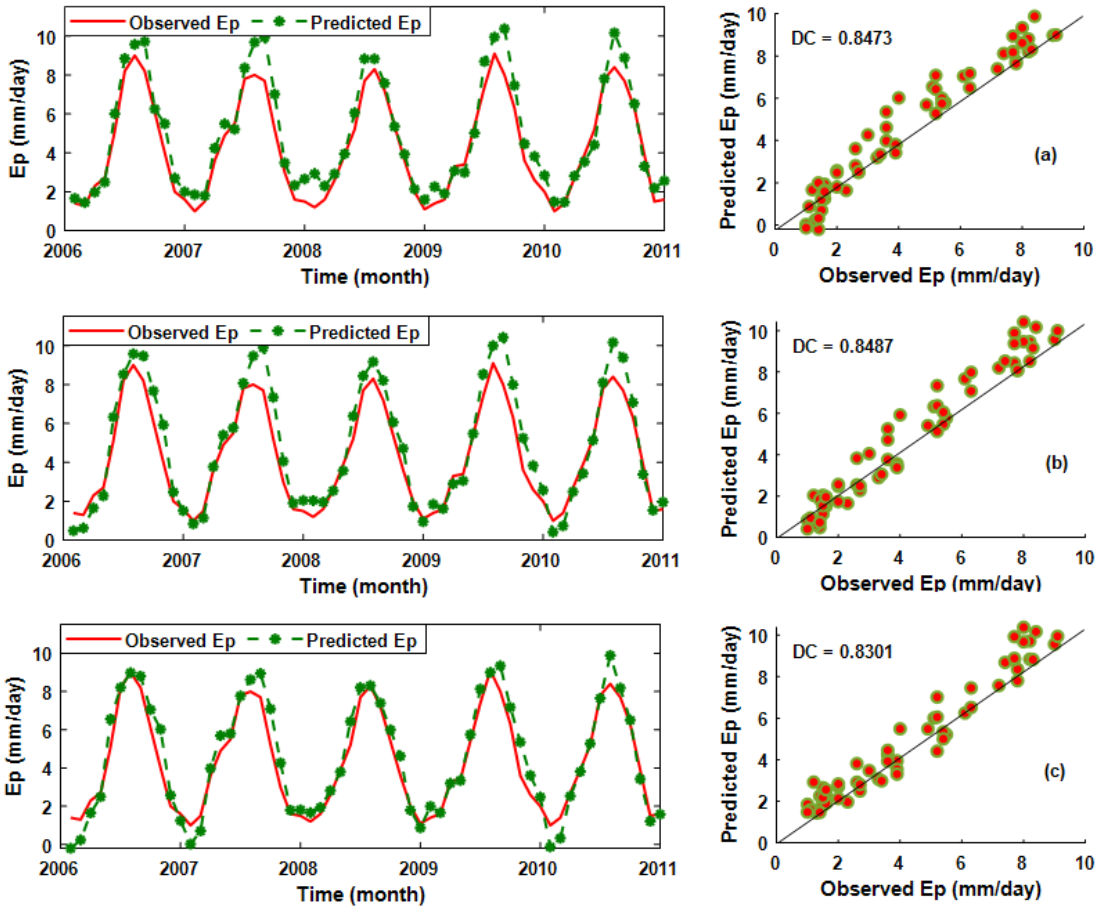

Figure 7: Time series and scatter plots for the best performance models in Salahaddin station for (a) ANN model (b) SVR model (c) MLR model

To further compare the performance of the models in both stations, Taylor diagrams are plotted. The overall models' performances are summarizing by Taylor diagram considering models variability, error (RMSE) between computed and observed data and pattern correlation (Mehr et al., 2019). The records similarity between predicted and observed models is ascertained based on correlation coefficient (R) and standard deviation (SD), while the distance from the reference (observed) point is measured by RMSE (Yaseen et al., (2019). Figures 8 and 9 show the Taylor diagrams demonstrating the performances of the best models in both Erbil and Salahaddin stations.

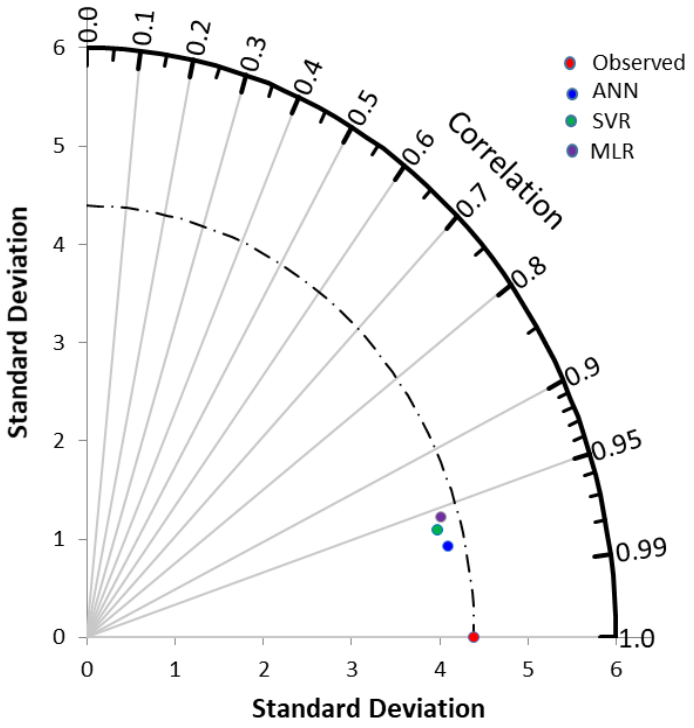

Figure 8: Taylor diagram demonstrating the performance of the applied models for Erbil station

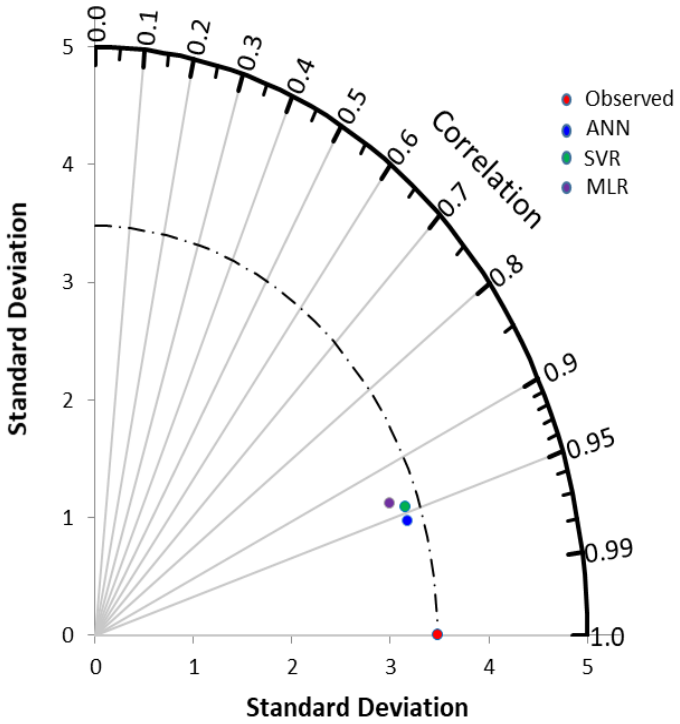

Figure 9. Taylor diagram demonstrating the performance of the applied models for Salahaddin station

It can be seen that in both stations, the AI based models show better performance than MLR model. For Erbil station, in terms of R, the performances of the models are 0.9757, 0.9646 and 0.9570 for ANN, SVR and MLR models, respectively. Similarly, for Salahaddin station, the performances of ANN, SVR and MLR models are 0.9564, 0.9449 and 0.9370, respectively. By observing the performances of the models with regard to their difference with the observed value, it can be deduced that the AI models are more close to the observed value which indicate better agreement between predicted and observed values and hence, superior performance.

4. Conclusion

In this study, the potentials of two AI and (ANN and SVR) and MLR models in prediction of pan evaporation in Erbil and Salahaddin stations of Iraq were ascertained using five different input combinations. Pearson correlation matrix was applied to determine the preferred inputs.

The results of the study showed that Temperatures (T_{max}, T_{min}, and T_{mean}) have higher correlation to Ep. The results also showed an increased performance of the applied models when the number of input variables increased which implied that, Ep depends on many factors for its prediction. The models demonstrated higher accuracy in Erbil station than Salahaddin station. The AI models performed better than MLR model, which most probably could be attributed to their ability to deal with nonlinear aspect of the system. ANN was found to have better performance for most of the developed models in both stations. Moreover, the results of this study implied that when the variables are properly utilized, the applied models in the study stations could achieve a successful modeling of ET_0. Thus, further studies should incorporate more stations and models different from those used in this study, to determine their performances.

References

Abdullahi, J., & Elkiran, G. (2017). Prediction of the future impact of climate change on reference evapotranspiration in Cyprus using artificial neural network. *Procedia* computer science, 120, 276-283.

Abdullahi, J., Elkiran, G., & Nourani, V. (2017). Application of Artificial Neural Network to predict reference evapotranspiration in Famagusta, North Cyprus. In *11th International Scientific Conference on Production Engineering Development and Modernization of Production* (pp. 549-554).

Azorin-Molina, C., Vicente-Serrano, S. M., Sanchez-Lorenzo, A., McVicar, T. R., Morán-Tejeda, E., Revuelto, J., & Tomas-Burguera, M. (2015). Atmospheric evaporative demand observations estimate and driving factors in Spain (1961–2011). *Journal of Hydrology*, *523*, 262-277.

Bewoor, M. L., Londhe, S. N., Kamble, A., Solanki, N., Nimbalkar, P., & Singh, N. (2016, March). Estimation of pan-evaporation using spatiotemporal data mining approach. In *National Conference NCPCI* (p. 19).

Cortes, C., & Vapnik, V. (1995). Support-vector networks Machine learning (pp. 237–297), Vol. 20.

Elkiran, G., Nourani, V., Abba, S. I., & Abdullahi, J. (2018). Artificial intelligence-based approaches for multi-station modelling of dissolve oxygen in river. *Global Journal of Environmental Science and Management*, *4*(4), 439-450.

Ghorbani, M. A., Deo, R. C., Yaseen, Z. M., Kashani, M. H., & Mohammadi, B. (2018). Pan evaporation prediction using a hybrid multilayer perceptron-firefly algorithm (MLP-FFA) model: case study in North Iran. *Theoretical and Applied Climatology*, *133*(3-4), 1119-1131.

Goyal, M. K., Bharti, B., Quilty, J., Adamowski, J., & Pandey, A. (2014). Modeling of daily pan evaporation in sub-tropical climates using ANN, LS-SVR, Fuzzy Logic, and ANFIS. *Expert Systems with Applications*, *41*(11), 5267-5276.

Haghiabi, A. H., Azamathulla, H. M., & Parsaie, A. (2017). Prediction of head loss on cascade weir using ANN and SVM. *ISH Journal of Hydraulic Engineering*, *23*(1), 102-110.

Hornik, K., Stinchcombe, M., & White, H. (1989). Multilayer feedforward networks are universal approximators. *Neural etworks*, *2*(5), 359-366.

Kim, S., Shiri, J., Singh, V. P., Kisi, O., & Landeras, G. (2015). Predicting daily pan evaporation by soft computing models with limited climatic data. *Hydrological Sciences Journal*, *60*(6), 1120-1136.

Kisi, O. (2015). Pan evaporation modeling using least square support vector machine, multivariate adaptive regression splines and M5 model tree. *Journal of Hydrology*, *528*, 312-320.

Legates, D. R., & McCabe Jr, G. J. (1999). Evaluating the use of "goodness- of- fit" measures in hydrologic and hydroclimatic model validation. *Water resources research*, *35*(1), 233-241.

Mehr, A. D., Nourani, V., Khosrowshahi, V. K., & Ghorbani, M. A. (2019). A hybrid support vector regression–firefly model for monthly rainfall forecasting. *International Journal of Environmental Science and Technology*, *16*(1), 335-346.

Nourani, V., Alami, M. T., & Aminfar, M. H. (2009). A combined neural-wavelet model for prediction of Ligvanchai watershed precipitation. *Engineering Applications of Artificial Intelligence*, *22*(3), 466-472.

Nourani, V., Sharghi, E., & Aminfar, M. H. (2012). Integrated ANN model for earthfill dam's seepage analysis: Sattarkhan Dam in Iran. *Artif. Intell. Research*, *1*(2), 22-37.

Nourani, V., Elkiran, G., & Abdullahi, J. (2019a). Multi-station artificial intelligence-based ensemble modeling of reference evapotranspiration using pan evaporation measurements. *Journal of Hydrology*, *577*, 123958.

Nourani, V., Elkiran, G., Abdullahi, J., & Tahsin, A. (2019b). Multi-region modeling of daily global solar radiation with artificial intelligence ensemble. *Natural Resources Research*, 1-22.

Qasem, S. N., Samadianfard, S., Kheshtgar, S., Jarhan, S., Kisi, O., Shamshirband, S., & Chau, K. W. (2019). Modeling monthly pan evaporation using wavelet support vector regression and wavelet artificial neural networks in arid and humid climates. *Engineering Applications of Computational Fluid Mechanics*, *13*(1), 177-187.

Rahimikhoob, A. (2009). Estimating daily pan evaporation using artificial neural network in a semi-arid environment. *Theoretical and Applied Climatology*, *98*(1-2), 101-105.

Rasul, A., Balzter, H., & Smith, C. (2015). Spatial variation of the daytime Surface Urban Cool Island during the dry season in Erbil, Iraqi Kurdistan, from Landsat 8. *Urban Climate*, *14*, 176-186.

Sarlak, N., & Agha, O. M. M. (2018). Spatial and temporal variations of aridity indices in Iraq. *Theoretical and Applied Climatology*, *133*(1-2), 89-99.

Sharghi, E., Nourani, V., & Behfar, N. (2018). Earthfill dam seepage analysis using ensemble artificial intelligence-based modeling. *Journal of Hydroinformatics*, *20*(5), 1071-1084.

Shiri, J., Marti, P., & Singh, V. P. (2014). Evaluation of gene expression programming approaches for estimating daily evaporation through spatial and temporal data scanning. *Hydrological Processes*, *28*(3), 1215-1225.

Shirsath, P. B., & Singh, A. K. (2010). A comparative study of daily pan evaporation estimation using ANN, regression and climate-based models. *Water Resources Management*, *24*(8), 1571-1581.

Valipour, M., & Eslamian, S. (2014). Analysis of potential evapotranspiration using 11 modified temperature-based models. *International Journal of Hydrology Science and Technology*, *4*(3), 192-207.

Wang, W. C., Xu, D. M., Chau, K. W., & Chen, S. (2013). Improved annual rainfall-runoff forecasting using PSO–SVM model based on EEMD. *Journal of Hydroinformatics*, *15*(4), 1377-1390.

Wang, L., Niu, Z., Kisi, O., Li, C. A., &Yu, D. (2017). Pan evaporation modeling using four different heuristic approaches. *Computers and Electronics in Agriculture*, *140*, 203-213.

Yang, H., & Yang, D. (2012). Climatic factors influencing changing pan evaporation across China from 1961 to 2001. *Journal of Hydrology*, *414*, 184-193.

Yaseen, Z. M., Ebtehaj, I., Kim, S., Sanikhani, H., Asadi, H., Ghareb, M. I., ... & Shahid, S. (2019). Novel hybrid data-intelligence model for forecasting monthly rainfall with uncertainty analysis. *Water*, *11*(3), 502.

Zhang, Q., Qi, T., Li, J., Singh, V. P., & Wang, Z. (2015). Spatiotemporal variations of pan evaporation in China during 1960–2005: changing patterns and causes. *International Journal of Climatology*, *35*(6), 903-912.